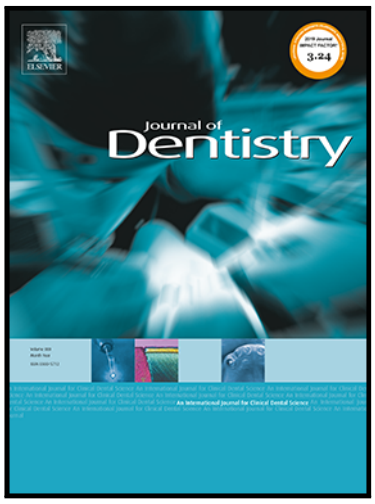

Surface characteristics, cytotoxicity, and microbial adhesion of 3D-printed hybrid resin-ceramic materials for definitive restoration

Suya Wang , Jingtao Dai , Shulan Xu , Ping Li ,
Ahmed Mahmoud Fouda , Burak Yilmaz , Abdulaziz Alhotan

PII: S0300-5712(24)00606-7
DOI: https://doi.org/10.1016/j.jdent.2024.105436
Reference: JJOD 105436

To appear in: *Journal of Dentistry*

Received date: 16 August 2024
Revised date: 23 October 2024
Accepted date: 24 October 2024

Please cite this article as: Suya Wang , Jingtao Dai , Shulan Xu , Ping Li , Ahmed Mahmoud Fouda , Burak Yilmaz , Abdulaziz Alhotan , Surface characteristics, cytotoxicity, and microbial adhesion of 3D-printed hybrid resin-ceramic materials for definitive restoration, *Journal of Dentistry* (2024), doi: https://doi.org/10.1016/j.jdent.2024.105436

Surface characteristics, cytotoxicity, and microbial adhesion of 3D-printed hybrid resin-ceramic materials for definitive restoration

Suya Wang [a], Jingtao Dai [b], Shulan Xu [a], Ping Li [c *], Ahmed Mahmoud Fouda [d e], Burak Yilmaz [f] Abdulaziz Alhotan [g]

a. Center of Oral Implantology, Stomatological Hospital, School of Stomatology, Southern Medical University, S366 Jiangnan Boulevard, Guangzhou 510280, China

b. Department of Orthodontics, Stomatological Hospital, School of Stomatology, Southern Medical University, S366 Jiangnan Boulevard, Guangzhou 510280, China

c. Department of Prosthodontics, School and Hospital of Stomatology, Guangdong Engineering Research Center of Oral Restoration and Reconstruction & Guangzhou Key Laboratory of Basic and Applied Research of Oral Regenerative Medicine, Guangzhou Medical University, Guangzhou, PR China.

d. Department of Oral Technology, Medical Faculty, University Hospital Bonn, 53111, Bonn, North Rhine-Westphalia, Germany

e. Department of Fixed Prosthodontics, Suez Canal University, Ismailia, Egypt.

f. Department of Reconstructive Dentistry and Gerodontology, School of Dental Medicine, University of Bern, Bern, Switzerland

g. Dental Health Department, College of Applied Medical Sciences, King Saud University, P.O. Box 10219, Riyadh 12372, Saudi Arabia

*** Corresponding authors:**

Ping Li, Ph.D.

Email: pingli@gzhmu.edu.cn

Acknowledgment

The authors acknowledge the financial support from the Science Research Cultivation Program of the Stomatological Hospital, Southern Medical University (PY2023002). Additionally, the authors thank the Researchers Supporting Project Number (RSPD2024R790), King Saud University, Riyadh, Saudi Arabia.

Abstract

Objective: This study investigated the surface properties, cytotoxicity, and microbial adhesion of 3D-printed specimens made from hybrid resin-ceramic materials intended for use in definitive crowns.

Methods: Disc-shaped specimens were 3D-printed using six different hybrid resin-ceramic materials recommended for definitive restorations: Crowntec (CT), VarseoSmile Crown Plus (VS), Tera Harz TC-80DP Graphy (TH), C&B Permanent ODS (CB), Formlabs Permanent Crown (FP), and HeyGears (HG). Surface topography, surface roughness, and water contact angle values were measured for each material (n = 6). Cytotoxicity was assessed using direct contact and extract tests on human gingival fibroblasts (n = 4). Additionally, the adhesion of mixed oral bacteria to the surfaces of the specimens was evaluated by counting colony-forming units (CFUs) after a 2-hour incubation period (n=6).

Results: The TH group exhibited significantly lower surface roughness (Ra: 0.28 ± 0.13 μm) compared to the other materials (CT: 1.87 ± 0.34 μm; VS: 1.13 ± 0.09 μm; CB: 2.91 ± 0.27 μm; FP: 2.50 ± 0.08 μm; HG: 1.50 ± 0.55 μm). The VS group had the highest water contact angle (129.5 ± 1.1°), indicating greater hydrophobicity, in contrast to the other groups (CT: 72.6 ± 2.1°; TH: 75.0 ± 0.3°; CB: 69.1 ± 0.2°; FP: 93.0 ± 1.6°; HG: 77.7 ± 0.3°). Cytotoxicity testing showed

no harmful effects, as relative cell viability exceeded 70%, and lactate dehydrogenase (LDH) release remained below 30% for all materials. The TH specimens also demonstrated the lowest bacterial adhesion.

Conclusions: The surface characteristics of the tested resin-ceramic materials varied significantly, with TH showing the smoothest surface and the least bacterial adhesion. All materials were found to be non-toxic. Therefore, TH material has the potential to provide definitive restorations with less microbial adhesion.

Clinical Significance: The type of resin-ceramic material significantly affects the surface properties of 3D-printed specimens. These findings are crucial for selecting the appropriate resin-ceramic material for definitive restorations.

Keywords: additive manufacturing, 3D-printing, surface characteristics, cytotoxicity, bacteria adhesion

1. Introduction

With advancements in digital dentistry, computer-aided design and computer-aided manufacturing (CAD/CAM) techniques have been become widely used across various dental fields [1,2]. In the realm of CAM, additive manufacturing (AM), commonly referred to as 3D printing, has been employed to create a variety of dental restorations, including artificial teeth, denture bases, temporary crowns, and bridges using polymers [3–5]. Recently, ceramic-reinforced composite resins with promising potential for definitive crowns have been developed and studied. These resin-based materials come into close contact with gingival tissues and interact with epithelial cells and fibroblasts [6]. The release of toxic chemical compounds due to progressive degradation or incomplete polymerization can impact adjacent tissues, potentially leading to local oral toxic effects [7,8]. Therefore, the proper attachment of these cells to biomaterials is essential to support cell migration, proliferation, and new tissue formation [9].

The most commonly used method for processing resin-ceramic materials is vat polymerization (VP), a 3D printing process that utilizes a light source to selectively polymerize the resin within a vat [10]. Depending on the printer's light source, VP printing is further categorized into stereolithography (SLA), direct light processing (DLP), or liquid crystal display (LCD) technologies [11,12]. The SLA process employs a liquid resin vat, a model-building platform, and an ultraviolet (UV) laser. The building platform is submerged in liquid resin and polymerized layer by layer using UV light [13]. While DLP AM and SLA technologies share many similarities, their main distinction lies in the light source: DLP printers use a projector or digital micromirror device to project a light mask, polymerizing an entire layer simultaneously [14]. LCD technology, on the other hand, uses light from LCD screens to polymerize the

photosensitive resin. In SLA printers, resolution is determined by the laser spot diameter, while in DLP and LCD technologies, it is defined by the pixel size of the projector or LCD screen [15]. The surface characteristics of 3D-printed restorations are known to play a critical role in bacterial adhesion [16]. Previous studies indicate that microorganisms prefer rougher surfaces, which offer protection against shear forces during initial attachment and provide a larger surface area for biofilm formation [16-18]. Various factors, including the composition of hybrid resin-ceramic materials, 3D printing technology, printing parameters, and polishing procedures, can affect the material's surface properties [18]. Dental materials science aims to develop restorative materials that inhibit microbial adhesion and colonization using different technologies. Since bacterial adhesion is the initial step in colonization that could lead to dental material-related infections, it is crucial to prevent this process to manage such infections [19]. However, a significant limitation of AM dentures is their suboptimal surface properties due to the layer-by-layer deposition approach [20,21]. Adjusting the physical and chemical properties of hybrid resin-ceramic materials is, therefore, vital for minimizing biofilm formation and preventing dental caries. While most research on 3D printing materials for restorative purposes has focused on physical and mechanical properties [22], dimensional accuracy, and optical characteristics [23–25], studies exploring surface characteristics, biological effects, and bacterial adhesion of 3D-printed hybrid resin-ceramic materials remain limited.

This study evaluated the effects of six hybrid resin-ceramic materials on surface characteristics, cytotoxicity, and microbial adhesion. Measurements of surface topography, roughness, and wettability were conducted. Additionally, cytotoxicity was assessed through extract and direct contact tests using human gingival fibroblasts (HGFs), while microbial adhesion was analyzed by counting colony-forming units. The null hypothesis of this study was three-fold: (i) different

hybrid resin-ceramic materials do not influence surface characteristics, (ii) they do not affect cytotoxicity, and (iii) they do not impact microbial adhesion.

2. Materials and Methods

2.1. Experimental design

Six hybrid resin-ceramic materials recommended for definitive dental restorations were selected for the current study: Crowntec (CT), VarseoSmile Crown Plus (VS), Tera Harz TC-80DP Graphy (TH), and C&B Permanent ODS (CB), all produced using the Sonic Mighty 4K printer (Phrozen, Hsinchu, Taiwan); Formlabs Permanent Crown (FP) by Formlabs Inc. (Somerville, MA, USA); and HeyGears (HG) using the UltraCraft DS printer (HeyGears, Guangzhou, China). The required minimal sample size for each test was determined based on an effect size of 0.80, with a power of 80% and a significance level of $\alpha = 0.05$. For both surface roughness and surface wettability tests, the calculated sample size was $n = 5$ ($N = 30$) for each test, with two additional specimens prepared for SEM observation. For the cytotoxicity test, the sample size was $n = 4$ ($N = 36$). For the bacterial adhesion test, the required sample size was $n = 5$ ($N = 35$). The specimens were printed to facilitate detailed studies on cytotoxicity, bacterial adhesion, and surface properties, as illustrated in Fig 1.

2.2. Specimen preparation

Six hybrid resin-ceramic materials were used in this study, each measuring 2 × 10 mm (as detailed in Tables 1 and 2). The manufacturers of these composite resins recommended using three specific types of 3D printers to fabricate the specimens. Four materials (CT, VS, TH, and CB) were printed with an open-source LCD 3D printer (Sonic Mighty 4K, Phrozen, Hsinchu, Taiwan). The fifth material (FP) was printed using the Form 3 SLA 3D printer (Formlabs Inc.,

Somerville, MA, USA), while the sixth material (HG) was printed using a DLP printer (UltraCraft DS, HeyGears, Guangzhou, China).

The specimens were designed using free, open-source software available at Tinkercad.com. The design files were then exported as STL files and transferred to the respective slicing software: Preform Software (Formlabs Inc., Somerville, MA, USA), Chitubox (Version 1.9.1, Phrozen, Hsinchu, Taiwan), or HeyGears (UltraCraft DS, HeyGears, Guangzhou, China). To ensure uniformity, the specimens were duplicated and standardized by positioning them on supports at a 90º angle during printing. The design files were sent to the respective 3D printers, and the printing process followed the guidelines recommended by each resin manufacturer. All layers were printed with a thickness of 50 μm, and each resin type was placed in a separate resin vat within the 3D printer.

After printing, the specimens underwent a five-minute cleaning procedure using a washing machine (Phrozen, Formlabs, or HeyGears) with a 99.5% isopropyl alcohol solution to remove any unpolymerized resin residue. After drying, the specimens (CT, VS, TH, CB, and FP) were exposed to a UV light-curing unit (Phrozen or Formlabs) for 20 minutes to facilitate further polymerization. The HG specimens were placed in an oven (HeyGears, China) at 120°C for 15 minutes (Table 3). Following post-processing, the supporting bars were removed, and the specimens were polished using silicon carbide sheets with grain sizes of P1200 and P2500 on a MetaServ 250 (Buehler, IL, USA).

2.3. Surface characterization

Surface roughness was evaluated using an optical profilometer (Bruker Contour GT K 3D, Billerica, USA) to analyze the topography of the different groups. Each group consisted of six specimens, which were measured using vertical scanning interferometry with a ×50

magnification lens and an additional ×0.55 optical magnification, a field of view of 230 × 170 μm, and a scan speed of 1 μm/s. The arithmetical mean height (Ra) was calculated, and surface topographies were reconstructed in 3D using Bruker Vision 64 V5.8.4 software (Bruker Corp., San Jose, USA).

Following 3D surface topography reconstruction, the specimens were sputter-coated with gold-palladium (SC7620, Laughton, East Sussex) and imaged using scanning electron microscopy (SEM) (MIRA4 LMH, TESCAN, Brno, Czech Republic) at magnifications of ×100, ×500, and ×2500 to characterize their surface morphology.

The hydrophilicity of each group was assessed through water contact angle (CA) measurements using a drop-shape analyzer (LSA100, Lauda Scientific, Germany). The automated dosing system deposited 2 μL water droplets at the center of each specimen's surface. After 20 seconds, a video camera aligned with the dosing needle captured the droplet deposition, and the contact angle was then measured and recorded.

2.4. Cytotoxicity test

Extract and direct contact tests were performed on human gingival fibroblasts (HGFs) to assess cytotoxicity, following ISO 10993-5:2009 and ISO 10993-12:2021 standards [26]. A titanium-based alloy (Ti-6Al-4V) was used as the negative control (NC), pure copper served as the positive control (PC), and cell culture medium without a specimen acted as the blank (BLK). HGFs were obtained from Procell Life Science and Technology (Wuhan, China) and cultured in Dulbecco's Modified Eagle Medium, supplemented with 10% fetal bovine serum and 1% penicillin/streptomycin (Life Technologies, UK), at 37°C in a 5% CO_2 atmosphere.

2.4.1. Extract test

The specimens were submerged in a medium at a surface area-to-medium ratio of 3.0 cm^2/mL for 72 hours, and the extracts were then sterilized by filtering through a 0.2 μm filter. HGFs were seeded overnight in 96-well plates at a cell density of 3×10^4 cells/cm^2. Following this, the respective specimen extracts were added, and the cells were incubated for an additional 24 hours. To assess cell membrane integrity, the cells were stained using a Calcein-AM and propidium iodide (PI) staining assay (KeyGEN BioTECH, China) and observed under a fluorescence microscope (DMi8, Leica, Wetzlar, Germany). Furthermore, the relative cell metabolic activity was evaluated using a Cell Counting Kit-8 assay (CCK-8, Glpbio, Montclair, CA, USA). Lastly, the relative lactate dehydrogenase (LDH) release was measured using an LDH cytotoxicity assay kit (Abcam, Shanghai, China), following the manufacturer's instructions.

2.4.2. Direct contact test

A direct contact test was conducted to further evaluate cytotoxicity. Four specimens from each group were processed simultaneously in 24-well culture plates. Cells were seeded onto the surface of the specimens at a density of 3×10^4 cells/cm^2. Following incubation, a Calcein-AM and PI staining assay (KeyGEN BioTECH, China) was used to examine cell membrane integrity under a fluorescence microscope (Leica, Wetzlar, Germany). Additionally, relative cell metabolic activity was assessed using a CCK-8 assay. To ensure reproducibility, the cytotoxicity tests were independently repeated three times.

2.5. Bacterial Strains and Growth Conditions

Following previous studies, a bacterial adhesion experiment was performed using a mixture of human oral bacteria to replicate denture-wearing conditions in the oral cavity [27]. Initially, mixed oral bacteria were freshly collected from human saliva and inoculated into a liquid brain-heart infusion (BHI) medium (BBL, BD, USA). The cultures were incubated in a 5% CO_2

environment for 24 hours. Before inoculating the surface of each specimen, the optical density of the bacterial suspension was adjusted to 0.54 at 620 nm, corresponding to 10^8 CFU/mL.

2.6. Bacterial adhesion test

Six samples from each group were prepared to investigate bacterial adhesion. After adjusting the bacterial suspension to 10^8 CFU/mL, 100 µL of this suspension was mixed with 1 mL of liquid BHI medium and added to the surface of each specimen. The wells were then incubated at 37°C for 2 hours. After incubation, the specimens were washed three times to remove any non-adherent bacteria.

Each specimen was then placed into a tube containing 1 mL of saline solution. The tubes were subjected to an ultrasonic cleaning bath (TE Laboratory Technology Co., LTD) at 50 kHz and 150 W for 1 minute, followed by agitation using a Vortex-Genie® 2 Mixer (Bohemia, New York, USA) to promote the detachment of adhered microorganisms. A series of four dilutions was performed by transferring 100 µL of this solution into 900 µL of saline solution. From Dilution 4, 50 µL was spread on a blood agar plate in duplicate and incubated at 37°C for 24 hours. After incubation, bacterial colonies were counted using an automatic colony counter (Interscience Scan 500, France) to measure colony-forming units (CFU) per millilitre.

2.7. Statistical analysis

All measurements were expressed as means ± standard deviations (SD). Statistical analyses were conducted using GraphPad Prism software (Version 9.5.0, La Jolla, CA, USA). A one-way analysis of variance (ANOVA) for repeated measurements was performed, followed by Tukey's multiple comparison tests. Results were considered statistically significant at $p < 0.05$.

3. Results

3.1 Surface characteristics

Fig. 2 shows the representative SEM images of the specimens at various magnifications. The CT and VS surfaces display a grid network formed by intersecting vertical and horizontal lines. At higher magnification (×2500), numerous particles were visible on both surfaces. In contrast, the TH specimens exhibited a clear and smooth surface even at high magnification (×2500). The CB group displayed a concave and convex striped surface, with small particles distributed within the concave regions. The FP and HG surfaces appeared relatively smoother compared to the CT, VS, and CB surfaces, although particles were still observed at higher magnification (×2500).

As depicted in Fig. 3a, the reconstructed 3D surface topographies were consistent with the SEM images, except for the concave stripes observed on the CB surface. Fig. 3b illustrates the Ra values of the different samples. A one-way ANOVA ($F [5, 12] = 31.06$, $p < 0.0001$) indicated significant differences in Ra values among the groups. Tukey's multiple comparison tests showed that the Ra values for the TH group (0.28 ± 0.13 μm) were significantly lower than those of all other groups ($p < 0.05$). The CB group had the highest Ra values (2.91 ± 0.27 μm), which were significantly greater than those in most other groups, except for the FP group (2.50 ± 0.08 μm) ($p = 0.55$). Additionally, the Ra values for the FP group were significantly higher than those in the VS (1.13 ± 0.09 μm) and HG (1.50 ± 0.55 μm) groups. No significant difference was observed between the CT (1.87 ± 0.34 μm) and VS groups ($p = 0.08$). Fig. 3c presents a heatmap of the p-values for surface roughness.

Fig. 4 displays the contact angles (CAs) for each group, revealing significant differences ($F [5, 12] = 18.95$, $p < 0.0001$). The Tukey's multiple comparisons test showed that the CA in the VS group ($129.5 \pm 1.1°$) was significantly higher than in all other groups. Additionally, the CA in the FP group ($93.0 \pm 1.6°$) was significantly higher than those in the TH ($75.0 \pm 0.3°$) and CB ($69.1 \pm 0.2°$) groups, with no significant differences between the TH, CB, and HG ($77.7 \pm 0.3°$) groups.

Although the FP specimens exhibited a more hydrophobic surface than the CT specimens (72.6 ± 2.1°), the difference was not statistically significant.

3.2. Cytotoxicity evaluation with HGFs

Fig. 5 and 6 display the cytotoxicity evaluation of human gingival fibroblasts (HGFs) using the extract test (Fig. 5) and direct contact test (Fig. 6). Fig. 5a presents live/dead images of HGFs exposed to the specimen extracts for 72 hours. Most cells in the extracts from the 3D-printed groups showed green fluorescence, indicating intact cell membranes. The cells maintained a spindle shape with distinct outlines, similar to those observed in the negative control, with no noticeable differences in cell density between the blank and negative controls.

The relative metabolic activity was assessed using the Cell Counting Kit-8 assay to quantify the extract test results. As shown in Fig. 5b, HGFs cultured in the extracts of 3D-printed specimens exhibited a relative metabolic activity exceeding 70% of the negative control. Additionally, the relative lactate dehydrogenase (LDH) release, depicted in Fig. 5c, was below 30% of the negative control for all groups. These findings indicate that the 3D-printed specimens did not exhibit cytotoxic effects in the extract test.

Fig. 6a shows HGFs cultured on the specimen surfaces, examined using a live/dead assay to assess the direct contact effects. Fibroblasts with elliptical morphology were randomly adhered to the surfaces of the 3D-printed specimens, similar to those observed in the negative controls. Most cells on the surfaces of the tested groups exhibited green fluorescence, indicating viability and intact cell membranes.

Fig. 6b illustrates the relative metabolic activity of HGFs cultured on the specimen surfaces. While the relative metabolic activity of HGFs exceeded 70% of the negative control, the mean

metabolic activities in the 3D-printed specimen groups were generally lower than in the negative controls.

Among the 3D-printed groups, the TH specimens showed significantly higher relative metabolic activity than the other groups, as shown in Fig. 6c ($p < 0.05$). The VS group had significantly lower relative metabolic activity compared to the CT, TH, HG, and CB groups. Although the VS group also trended towards lower activity than the FP group, this difference did not reach statistical significance ($p = 0.05$). Overall, these results suggest that the 3D-printed specimens influenced biocompatibility, as indicated by the lower cell viability compared to the control group, with the TH specimens demonstrating the least cytotoxicity.

3.3. Microbial adhesion

The adhesion of the oral bacteria mixture to the specimen surfaces was evaluated using colony counting methods (Fig. 7). Significant differences in colony count values were observed between the groups ($F [6, 11] = 3.307$, $p < 0.05$). The Tukey's multiple comparison test indicated that the CB group had the highest CFU counts, while the TH specimen surfaces exhibited the lowest number of colonies.

Fig. 7b illustrates the statistical distribution of mean and standard deviation values for oral bacterial adhesion. The CB group demonstrated significantly higher bacterial counts compared to the TH group, with a trend towards higher CFU counts than those found in the CT, VS, FP, HG, and control (Ti) groups; however, these differences were not statistically significant. Additionally, Tukey's multiple comparisons analysis revealed that the TH group had significantly lower bacterial counts than all other 3D-printed specimen groups. Overall, these results suggest that TH specimens have a greater potential to reduce oral bacterial adhesion on their surfaces.

4. Discussion

This study investigated the impact of different resin-ceramic materials fabricated using various 3D printing technologies on surface characteristics, cytotoxicity, and bacterial adhesion. The results revealed that the TH specimens had a significantly lower Ra value than the other 3D-printed specimens, while the VS group exhibited the highest water contact angle. Therefore, the first hypothesis that different hybrid resin-ceramic materials do not influence surface characteristics was rejected. The second hypothesis that these materials do not affect cytotoxicity was accepted, as all six resin-ceramic materials showed no cytotoxic effects. However, the third hypothesis that different hybrid resin-ceramic materials do not affect microbial adhesion was rejected, as quantitative results showed significantly lower bacterial adhesion in the TH group compared to the others.

The surface characteristics of 3D-printed dental restorations vary depending on the 3D printing technology, printing parameters, and the materials used. The resin-based materials evaluated in this study differed in terms of the chemical composition of their polymer matrices and initiator systems (Tables 1 and 2). The TH specimens displayed relatively smooth surfaces, while the CB specimens had the highest surface roughness (Figs. 2 and 3). Variations in the chemical compositions of these resin materials likely explain these observations. During the initial curing phase, light or laser irradiation triggers photoinitiator reactions, bonding unlinked monomers into a polymer, which forms the primary surface texture [28]. This process highlights the significant role of resin matrix components in influencing surface roughness, aligning with our findings.

Despite differences in their initiator systems, CT and VS share the same resin matrix and printing process, using the same device. Consequently, their surface roughness showed no significant differences, likely due to the polymerization mechanism of the 3D-printed photosensitive resin

not impacting surface roughness. Previous research also indicates that different post-curing methods do not significantly alter the surface roughness of 3D-printed denture base materials [29]. Composite resins exhibit varying water contact angles based on their composition. In this study, the VS specimens showed a significantly higher contact angle (129.5 ± 1.1°) than the CT specimens (72.6 ± 2.1°). Fumed silica was the only component that differed between the two resin systems, potentially explaining this difference. Fumed silica (pyrogenic silica) is hydrophilic. Sergey Savotchenko et al. observed that the introduction of pyrogenic silica could increase water absorption. Their study showed that incorporating polydimethylsiloxane reduced the contact angle by 13% on a metal background. However, when both polydimethylsiloxane and a pyrogenic silica gel modifier were added, the contact angle decreased by 34% on the metal background [30].

Viscosity, an intrinsic property of resin, also affects surface roughness [23,24]. In this study, two polyurethane acrylate-based resins were used: TH (viscosity of ~2000 ± 300 cP) and CB (viscosity of ~150 ± 100 cP). The TH specimens had the lowest Ra value. In contrast, the CB specimens had the highest (Fig. 3). These results differ from previous findings, which reported that low-viscosity resins had the highest trueness and high-viscosity resins had the lowest [23]. This inconsistency may stem from differences in printing technologies, as the previous study used DLP printing [23], whereas this study employed LCD printing.

Biocompatibility is essential for 3D-printed dental materials used in medical devices [31]. A systematic review has shown that the cytotoxicity of resin-based materials is influenced by factors such as monomers, filler particles, additives, and polymerization systems [32]. The degree of conversion in a composite resin plays a critical role in its cytotoxicity, as unreacted monomers can have significant biological effects [33]. All tested products theoretically pose no

toxicity risk, given that both the composition and degree of conversion of these resins are adequate.

HGFs were chosen as the target cells since they are the primary cells in contact with resin-based restorative materials in clinical settings [34]. During the preparation of deep cavities reaching the gingival sulcus, the gingival epithelium may be disrupted, leading the restorative materials to interact with gingival fibroblasts, which are crucial for healing.

Cell viability assays with eluates were performed according to ISO standards (ISO10993–5:2009;10993–12:2021) [26] Our findings showed high HGF viability (cell viability >70% of negative controls; LDH release <30% of negative controls) for 3D-printed materials, indicating an adequate degree of conversion with no cytotoxicity (Fig. 5).

In direct contact tests, HGFs displayed a greater affinity for smooth or finely grooved surfaces [35], as confirmed by the relatively high cell attachment on the TH surface (Fig. 6a). Surface wettability also affects cell proliferation, with hydrophilic surfaces promoting extracellular matrix protein adsorption, influencing cell activity [36]. The decrease in cell viability on the VS surface may be due to its hydrophobic nature and high contact angle (Fig. 3c). Similar results have been observed in studies comparing implant provisional resin materials, where more hydrophobic surfaces exhibited lower cell attachment and viability [37].

Bacterial adhesion is the first step in biofilm formation, which can compromise the clinical success of dental restorations [38]. Surface properties, including roughness [39,40], hydrophobicity [41], and free energy [42], can influence bacterial adhesion. However, there is no clear consensus in the literature on the impact of these factors due to the complex interplay of physical and chemical interactions [43 Additionally, some studies have reported conflicting results, finding no correlation between surface roughness and bacterial adhesion [44,45]. This

study revealed that the TH specimens exhibited the lowest bacterial adhesion, while CB showed the highest. This difference can be attributed to the smoother surface of the TH specimens and the rougher surface of the CB specimens. This is consistent with previous studies that found that increased surface roughness correlates with enhanced bacterial adhesion [46–48]. The observed increase in bacterial adhesion on rougher materials may be due to the roughness values of the CB specimens (2.9 μm) exceeding and the TH specimens (0.2 μm) meeting the threshold value. Moreover, a strong correlation was observed between surface roughness and bacterial counts ($r = 0.83$), indicating that roughness significantly influenced bacterial adhesion.

In addition to the impact of surface roughness on bacterial adhesion [49], wettability is another critical factor in microbial adherence [50]. A contact angle greater than 62° indicates hydrophobicity [51]. In this study, all six materials exhibited hydrophobic surfaces with contact angles above 62°. Despite the VS group having the highest contact angle, its CFU counts were similar to other groups, aligning with studies that found no significant relationship between hydrophobicity and bacterial adhesion [52,53]. No significant correlation ($r = 0.25$) was found between water contact angle and bacterial adhesion in this study.

In terms of clinical significance, the resin matrix and filler particle proportions strongly influence the surface characteristics of resin-ceramic materials, highlighting the importance of selecting appropriate materials and following manufacturer protocols to ensure quality. This study found that TH materials are more favourable for soft tissue management and exhibit reduced bacterial adhesion, making them suitable for fabricating definitive crowns.

However, this study evaluated a limited number of materials. Further investigation of different materials from various manufacturers is needed for a more comprehensive comparison. Additionally, only one type of printer was used per resin material, as mandated by the

manufacturer, limiting the assessment of the effects of different printers (LCD, SLA, DLP) on the resin. Finally, the impact of free surface energy on bacterial adhesion was not investigated, which warrants further research.

5. Conclusion

The results demonstrated that different resin-ceramic materials significantly affected surface characteristics, subsequently influencing bacterial adhesion. The TH specimens exhibited the smoothest surface and the lowest bacterial adhesion, highlighting their potential effectiveness for long-term provisional dental restorations in clinical applications.

6.Conflict of Interest

The authors report no conflict of interest regarding this manuscript.

	Material	Abbr.	Manufacturer	Manufacturing technique
Permanent resin	Crowntec™	CT	Saremco, Switzerland	Additive manufacturing technologies: liquid crystal display (LCD) 3D printer (Sonic Mighty 4K, Phrozen, Hsinchu, Taiwan).
	VarseoSmile Crown Plus™	VS	Bego, Bremen, Germany	
	Tera Harz TC-80DP™	TH	Graphy, Seoul, Korea	
	C&B Permanent™	CB	ODS, Seoul, Korea	
	Formlabs Permanent Crown™	FP	Formlabs, Somerville, MA, USA	Additive manufacturing technologies: Form 3 stereolithography (SLA) 3D printer (Formlabs Inc., Somerville, MA, USA).
	HeyGears™	HG	HeyGears, China	Additive Manufacturing technologies: digital light processing (DLP)

Table 1. 3D-printed hybrid resin-ceramic material used in the current study.

Table 2. Types and chemical compositions of the tested materials according to the manufacturers.

Material	Type	Matrix components	Fillers	Polymerization
CT	Nanohybrid composite	Esterification products of 4,4′-isopropylidiphenol, ethoxylated and 2-methylprop-2enoic acid	30–50 wt%. (silanized dental glass, pyrogenic silica, particle size 0.7 μm)	initiators
VS	Nanohybrid composite	Esterification products of 4,4′-isopropylidiphenol, ethoxylated and 2-methylprop-2enoic acid	30–50 wt%. (silanized dental glass, particle size 0.7 μm)	TPO; MBF
TH	polyurethane-based resin	Urethane acrylate oligomer, bisphenol A ethoxylate dimethacrylate, 2-HEMA, diphenyl (2,4,6-trimethylbenzoyl) phosphine oxide, and additives	N/A	TPO
CB	polyurethane-based resin	Diurethane dimethacrylate, 2-Propenoic acid, 2-methyl-, (1-methylethylidene) bis (4,1-phenyleneoxy(1-methyl-2,1-ethanediyl)) ester, 2-HEMA, diphenyl (2,4,6-trimethylbenzoyl) phosphine oxide, and additives	N/A	TPO
FP	Nanohybrid composite	Esterification products of 4,4′-isopropylidiphenol, ethoxylated and 2-	30–50 wt%. (silanized dental glass, particle size 0.7 μm)	TPO

		methylprop-2enoic acid; Bis-EMA,		
HG	Nanohybrid composite	7,7,9-trimethyl-4,13-dioxo- 3,14-dioxa-5,12-diazahexadecane-1, 16-diyl bismethacrylate	20–30 wt%. (Silicon dioxide)	2-PEA

Table 3. Post-processing and finishing steps of each tested material according to the manufacturer's protocol.

	Material	Post-processing and finishing steps
Permanent resin	CT	5 min ultrasonic cleaning with 99.5% isopropyl alcohol solution using a washing machine (Phrozen, Hsinchu, Taiwan), 20 min UV post-polymerization (Phrozen, Hsinchu, Taiwan), polishing with silicon carbide sheets using the MetaServ 250 (Buehler, IL, USA)
	VS	
	TH	
	CB	
	FP	5 min ultrasonic cleaning with 99.5% isopropyl alcohol solution using the Form Wash (Formlabs, Somerville, MA, USA), 20 min UV post-polymerization (Formlabs, Somerville, MA, USA), polishing with silicon carbide sheets using the MetaServ 250 (Buehler, IL, USA)
	HG	3 min ultrasonic cleaning with 99.5% isopropyl alcohol solution using a washing machine (HeyGears, Guangzhou, China), 15 min oven baking at 120 degree (HeyGears, Guangzhou, China), polishing with silicon carbide sheets using the MetaServ 250 (Buehler, IL, USA)

Reference

[1] N.Z. Baba, B.J. Goodacre, C.J. Goodacre, F. Müller, S. Wagner, CAD/CAM Complete Denture Systems and Physical Properties: A Review of the Literature, J. Prosthodont. 30 (2021) 113–124, https://doi.org/10.1111/jopr.13243.

[2] E.D. Rekow, Digital dentistry: The new state of the art - Is it disruptive or destructive?, Dent. Mater. 36 (2020) 9–24, https://doi.org/10.1016/j.dental.2019.08.103.

[3] E. Anadioti, L. Musharbash, M.B. Blatz, G. Papavasiliou, P. Kamposiora, 3D printed complete removable dental prostheses: a narrative review, BMC. Oral. Health. 20 (2020) 343, https://doi.org/10.1186/s12903-020-01328-8.

[4] P. Li, P.K. Fernandez, S. Spintzyk, F. Schmidt, J. Yassine, F. Beuer, A. Unkovskiy, Effects of layer thickness and build angle on the microbial adhesion of denture base polymers manufactured by digital light processing, J. Prosthodont. Res. 67 (2023) 562–567, https://doi.org/10.2186/jpr.JPR_D_22_00126.

[5] R. Galante, C.G. Figueiredo-Pina, A.P. Serro, Additive manufacturing of ceramics for dental applications: A review, Dent. Mater. 35 (2019) 825–846, https://doi.org/10.1016/j.dental.2019.02.026.

[6] S. Himmelsbach, T. Steinberg, P. Tomakidi, M. Garcia-Käufer, E. Hellwig, O. Polydorou, Effect of dental composite dust on human gingival keratinocytes, Dent. Mater. 39 (2023) 994–1003, https://doi.org/10.1016/j.dental.2023.09.004.

[7] M. Fujioka-Kobayashi, R.J. Miron, A. Lussi, R. Gruber, N. Ilie, R.B. Price, G. Schmalz, Effect of the degree of conversion of resin-based composites on cytotoxicity, cell attachment, and gene expression, Dent. Mater. 35 (2019) 1173–1193, https://doi.org/10.1016/j.dental.2019.05.015.

[8] M. Folwaczny, R. Ahantab, A. Kessler, C. Ern, I. Frasheri, Cytotoxicity of 3D printed resin materials for temporary restorations on human periodontal ligament (PDL-hTERT) cells, Dent. Mater. 39 (2023) 529–537, https://doi.org/10.1016/j.dental.2023.04.003.

[9] H. Schweikl, R. Müller, C. Englert, K.-A. Hiller, R. Kujat, M. Nerlich, G. Schmalz, Proliferation of osteoblasts and fibroblasts on model surfaces of varying roughness and surface chemistry, J. Mater. Sci. Mater. Med. 18 (2007) 1895–1905, https://doi.org/10.1007/s10856-007-3092-8.

[10] A.-L. Lambart, A.B. Xepapadeas, B. Koos, P. Li, S. Spintzyk, Rinsing postprocessing procedure of a 3D-printed orthodontic appliance material: Impact of alternative post-rinsing solutions on the roughness, flexural strength and cytotoxicity, Dent. Mater. 38 (2022) 1344–1353, https://doi.org/10.1016/j.dental.2022.06.010.

[11] A. Alammar, J.C. Kois, M. Revilla-León, W. Att, Additive Manufacturing Technologies: Current Status and Future Perspectives, J. Prosthodont. 31 (2022) 4–12, https://doi.org/10.1111/jopr.13477.

[12] V. Grassia, V. Ronsivalle, G. Isola, L. Nucci, R. Leonardi, A. Lo Giudice, Accuracy (trueness and precision) of 3D printed orthodontic models finalized to clear aligners production, testing crowded and spaced dentition, BMC. Oral. Health. 23 (2023) 352, https://doi.org/10.1186/s12903-023-03025-8.

[13] H. Kodama, Automatic method for fabricating a three-dimensional plastic model with photo-hardening polymer, Rev. Sci. Instrum. 52 (1981) 1770–1773, https://doi.org/10.1063/1.1136492.

[14] T.J. Horn, O.L.A. Harrysson, Overview of current additive manufacturing technologies and selected applications, Sci. Prog. 95 (2012) 255–282, https://doi.org/10.3184/003685012X13420984463047.

[15] W. Piedra-Cascón, V.R. Krishnamurthy, W. Att, M. Revilla-León, 3D printing parameters, supporting structures, slicing, and post-processing procedures of vat-polymerization additive manufacturing technologies: A narrative review, J. Dent. 109 (2021) 103630, https://doi.org/10.1016/j.jdent.2021.103630.

[16] A. Ionescu, E. Wutscher, E. Brambilla, S. Schneider-Feyrer, F.J. Giessibl, S. Hahnel, Influence of surface properties of resin-based composites on in vitro Streptococcus mutans biofilm development, Eur. J. Oral. Sci. 120 (2012) 458–465, https://doi.org/10.1111/j.1600-0722.2012.00983.x.

[17] J.W. Park, C.W. Song, J.H. Jung, S.J. Ahn, J.L. Ferracane, The effects of surface roughness of composite resin on biofilm formation of Streptococcus mutans in the presence of saliva, Oper. Dent. 37 (2012) 532–539, https://doi.org/10.2341/11-371-L.

[18] M. Ono, T. Nikaido, M. Ikeda, S. Imai, N. Hanada, J. Tagami, K. Matin, Surface properties of resin composite materials relative to biofilm formation, Dent. Mater. J. 26 (2007) 613–622, https://doi.org/10.4012/dmj.26.613.

[19] Y. Tu, H. Ren, Y. He, J. Ying, Y. Chen, Interaction between microorganisms and dental material surfaces: general concepts and research progress, J. Oral. Microbiol. 15 (2023) 2196897, https://doi.org/10.1080/20002297.2023.2196897.

[20] A. KEßLER, R. Hickel, N. Ilie, *In vitro* investigation of the influence of printing direction on the flexural strength, flexural modulus and fractographic analysis of 3D-printed temporary materials, Dent. Mater. J. 40 (2021) 641–649, https://doi.org/10.4012/dmj.2020-147.

[21] J. Dai, P. Li, S. Spintzyk, C. Liu, S. Xu, Influence of additive manufacturing method and build angle on the accuracy of 3D-printed palatal plates, J. Dent. 132 (2023) 104449, https://doi.org/10.1016/j.jdent.2023.104449.

[22] Y.-J. Kang, H. Kim, J. Lee, Y. Park, J.-H. Kim, Effect of airborne particle abrasion treatment of two types of 3D-printing resin materials for permanent restoration materials on flexural strength, Dent. Mater. 39 (2023) 648–658, https://doi.org/10.1016/j.dental.2023.05.007.

[23] N. Alharbi, R. Osman, D. Wismeijer, Effects of build direction on the mechanical properties of 3D-printed complete coverage interim dental restorations, J. Prosthet. Dent. 115 (2016) 760–767, https://doi.org/10.1016/j.prosdent.2015.12.002.

[24] C. Espinar, A. Della Bona, M. Tejada-Casado, R. Pulgar, M.M. Pérez, Optical behavior of 3D-printed dental restorative resins: Influence of thickness and printing angle, Dent. Mater. 39 (2023) 894–902, https://doi.org/10.1016/j.dental.2023.08.003.

[25] K. Luo, Q. Liu, A. Alhotan, J. Dai, A. Li, S. Xu, P. Li, Effect of post-curing conditions on surface characteristics, physico–mechanical properties, and cytotoxicity of a 3D-printed denture base polymer, Dent. Mater. 40(2024) 500-507, https://doi.org/10.1016/j.dental.2023.12.017.

[26] ISO 25178-2:2021, https://www.iso.org/standard/74591.html (accessed December 6, 2023).

[27] J. Dai, K. Luo, S. Spintzyk, A. Unkovskiy, P. Li, S. Xu, P.K. Fernandez, Post-processing of DLP-printed denture base polymer: Impact of a protective coating on the surface characteristics, flexural properties, cytotoxicity, and microbial adhesion, Dent. Mater. 38 (2022), https://doi.org/10.1016/j.dental.2022.11.008.

[28] J.W. Stansbury, M.J. Idacavage, 3D printing with polymers: Challenges among expanding options and opportunities, Dent. Mater. 32 (2016) 54–64, https://doi.org/10.1016/j.dental.2015.09.018.

[29] P. Li, A.-L. Lambart, B. Stawarczyk, M. Reymus, S. Spintzyk, Postpolymerization of a 3D-printed denture base polymer: Impact of post-curing methods on surface characteristics, flexural strength, and cytotoxicity, J. Dent 115 (2021) 103856, https://doi.org/10.1016/j.jdent.2021.103856.

[30] S. Savotchenko, E. Kovaleva, A. Cherniakov, Effect of epoxy resin modifications with industrial fillers on wetting and water absorption, Colloid. Polym. Sci. 301 (2023) 1–8, https://doi.org/10.1007/s00396-023-05061-w.

[31] F. Alifui-Segbaya, J. Bowman, A.R. White, S. Varma, G.J. Lieschke, R. George, Toxicological assessment of additively manufactured methacrylates for medical devices in dentistry, Acta. Biomater. 78 (2018) 64–77, https://doi.org/10.1016/j.actbio.2018.08.007.

[32] K. Wiertelak-Makała, I. Szymczak-Pajor, K. Bociong, A. Śliwińska, Considerations about Cytotoxicity of Resin-Based Composite Dental Materials: A Systematic Review, Int. J. Mol. Sci. 25 (2023) 152. doi: 10.3390/ijms25010152.

[33] H. Schweikl, G. Spagnuolo, G. Schmalz, Genetic and Cellular Toxicology of Dental Resin Monomers, J. Dent. Res. 85 (2006) 870–877, https://doi.org/10.1177/154405910608501001.

[34] K. Moharamzadeh, R. Van Noort, I.M. Brook, A.M. Scutt, Cytotoxicity of resin monomers on human gingival fibroblasts and HaCaT keratinocytes, Dent. Mater. 23 (2007) 40–44, https://doi.org/10.1016/j.dental.2005.11.039.

[35] S. Tetè, V.L. Zizzari, B. Borelli, M.D. Colli, S. Zara, R. Sorrentino, A. Scarano, E. Gherlone, A. Cataldi, F. Zarone, Proliferation and adhesion capability of human gingival fibroblasts onto zirconia, lithium disilicate and feldspathic veneering ceramic *in vitro* , Dent. Mater. J. 33 (2014) 7–15, https://doi.org/10.4012/dmj.2013-185.

[36] T.G. Ruardy, J.M. Schakenraad, H.C. van der Mei, H.J. Busscher, Adhesion and spreading of human skin fibroblasts on physicochemically characterized gradient surfaces, J. Biomed. Mater. Res. 29 (1995) 1415–1423, https://doi.org/10.1002/jbm.820291113.

[37] J. Shim, H. Kim, S. Park, H. Yun, J. Ryu, Comparison of Various Implant Provisional Resin Materials for Cytotoxicity and Attachment to Human Gingival Fibroblasts, Int. J. Oral. Maxillofac. Implants. 34 (2019) 390–396, https://doi.org/10.11607/jomi.6707.

[38] H.J. Busscher, R. Bos, H.C. van der Mei, Initial microbial adhesion is a determinant for the strength of biofilm adhesion, FEMS. Microbiol. Lett. 128 (1995) 229–234, https://doi.org/10.1111/j.1574-6968.1995.tb07529.x.

[39] K. Yang, J. Shi, L. Wang, Y. Chen, C. Liang, L. Yang, L.-N. Wang, Bacterial anti-adhesion surface design: Surface patterning, roughness and wettability: A review, J. Mater. Sci. Technol. 99 (2022) 82–100, https://doi.org/10.1016/j.jmst.2021.05.028.

[40] C. Echeverria, M.D.T. Torres, M. Fernández-García, C. de la Fuente-Nunez, A. Muñoz-Bonilla, Physical methods for controlling bacterial colonization on polymer surfaces, Biotechnol, Adv. 43 (2020) 107586, https://doi.org/10.1016/j.biotechadv.2020.107586.

[41] Y. Yuan, M. P. Hays, P. R. Hardwidge, J. Kim, Surface characteristics influencing bacterial adhesion to polymeric substrates, RSC. Adv. 7 (2017) 14254–14261, https://doi.org/10.1039/C7RA01571B.

[42] V. Carniello, B.W. Peterson, H.C. van der Mei, H.J. Busscher, Physico-chemistry from initial bacterial adhesion to surface-programmed biofilm growth, Adv. Colloid. Interface. Sci. 261 (2018) 1–14, https://doi.org/10.1016/j.cis.2018.10.005.

[43] R. Buergers, W. Schneider-Brachert, S. Hahnel, M. Rosentritt, G. Handel, Streptococcal adhesion to novel low-shrink silorane-based restorative, Dent. Mater. 25 (2009) 269–275, https://doi.org/10.1016/j.dental.2008.07.011.

[44] J.S. Shim, J.-E. Kim, S.H. Jeong, Y.J. Choi, J.J. Ryu, Printing accuracy, mechanical properties, surface characteristics, and microbial adhesion of 3D-printed resins with various printing orientations, J. Prosthet. Dent. 124 (2020) 468–475, https://doi.org/10.1016/j.prosdent.2019.05.034.

[45] P. Li, P.K. Fernandez, S. Spintzyk, F. Schmidt, F. Beuer, A. Unkovskiy, Effect of additive manufacturing method and build angle on surface characteristics and *Candida albicans* adhesion to 3D printed denture base polymers, J. Dent. 116 (2022) 103889, https://doi.org/10.1016/j.jdent.2021.103889.

[46] D.P. Bakker, H.J. Busscher, J. van Zanten, J. de Vries, J.W. Klijnstra, H.C. van der Mei, Multiple linear regression analysis of bacterial deposition to polyurethane coatings after conditioning film formation in the marine environment, Microbiology (Reading). 150 (2004) 1779–1784, https://doi.org/10.1099/mic.0.26983-0.

[47] H.J. Busscher, M. Rinastiti, W. Siswomihardjo, H.C. van der Mei, Biofilm formation on dental restorative and implant materials, J. Dent. Res. 89 (2010) 657–665, https://doi.org/10.1177/0022034510368644.

[48] M. Kozmos, P. Virant, F. Rojko, A. Abram, R. Rudolf, P. Raspor, A. Zore, K. Bohinc, Bacterial Adhesion of Streptococcus mutans to Dental Material Surfaces, Molecules. 26 (2021) 1152, https://doi.org/10.3390/molecules26041152.

[49] M. Fiedot-Toboła, M. Ciesielska, I. Maliszewska, O. Rac-Rumijowska, P. Suchorska-Woźniak, H. Teterycz, M. Bryjak, Deposition of Zinc Oxide on Different Polymer Textiles and Their Antibacterial Properties, Materials (Basel). 11 (2018) 707, https://doi.org/10.3390/ma11050707.

[50] S. BinAhmed, A. Hasane, Z. Wang, A. Mansurov, S. Romero-Vargas Castrillón, Bacterial Adhesion to Ultrafiltration Membranes: Role of Hydrophilicity, Natural Organic Matter, and Cell-Surface Macromolecules, Environ. Sci. Technol. 52 (2018) 162–172, https://doi.org/10.1021/acs.est.7b03682.

[51] E.A. Vogler, Structure and reactivity of water at biomaterial surfaces, Adv. Colloid. Interface. Sci. 74 (1998) 69–117, https://doi.org/10.1016/S0001-8686(97)00040-7.

[52] H. Tang, A. Wang, X. Liang, T. Cao, S.O. Salley, J.P. McAllister, K.Y.S. Ng, Effect of surface proteins on *Staphylococcus Epidermidis* adhesion and colonization on silicone, Colloids. Surf. B. Biointerfaces. 51 (2006) 16–24, https://doi.org/10.1016/j.colsurfb.2006.04.011.

[53] M. Gyo, T. Nikaido, K. Okada, J. Yamauchi, J. Tagami, K. Matin, Surface response of fluorine polymer-incorporated resin composites to cariogenic biofilm adherence, Appl. Environ. Microbiol. 74 (2008) 1428–1435, https://doi.org/10.1128/AEM.02039-07.

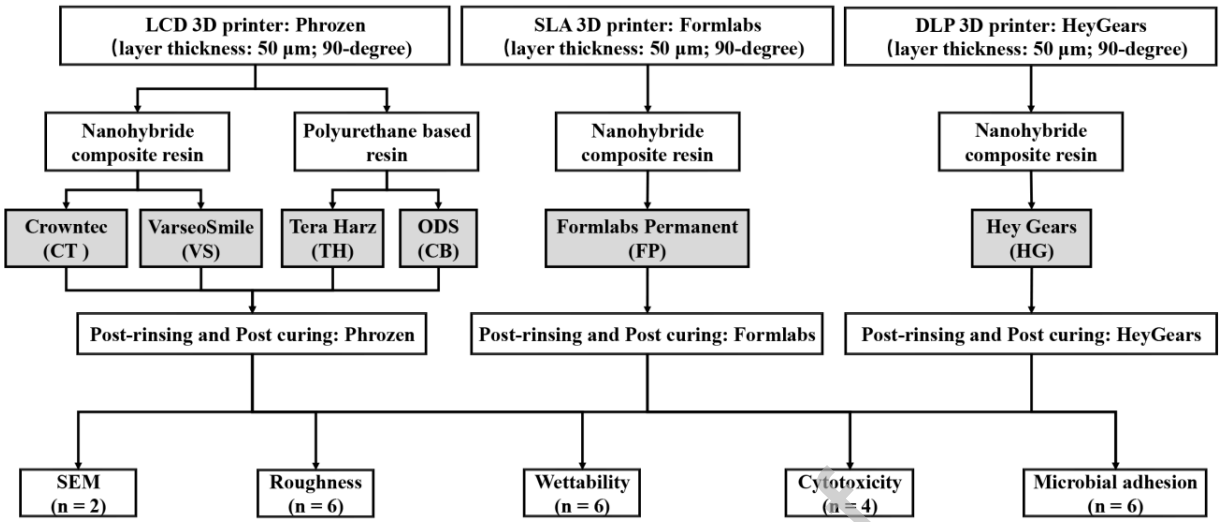

Fig 1

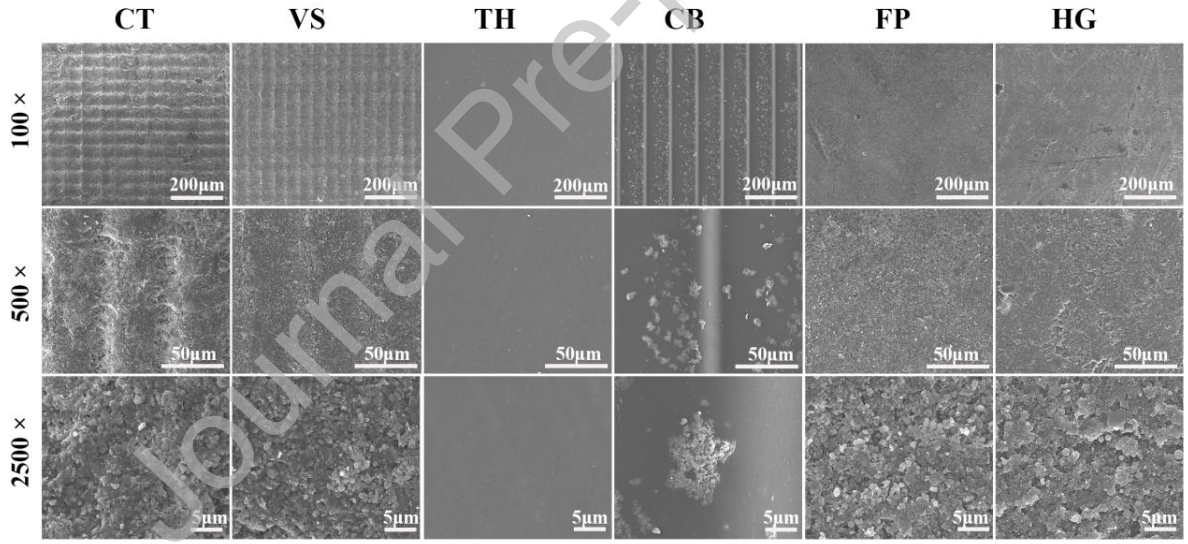

Fig 2

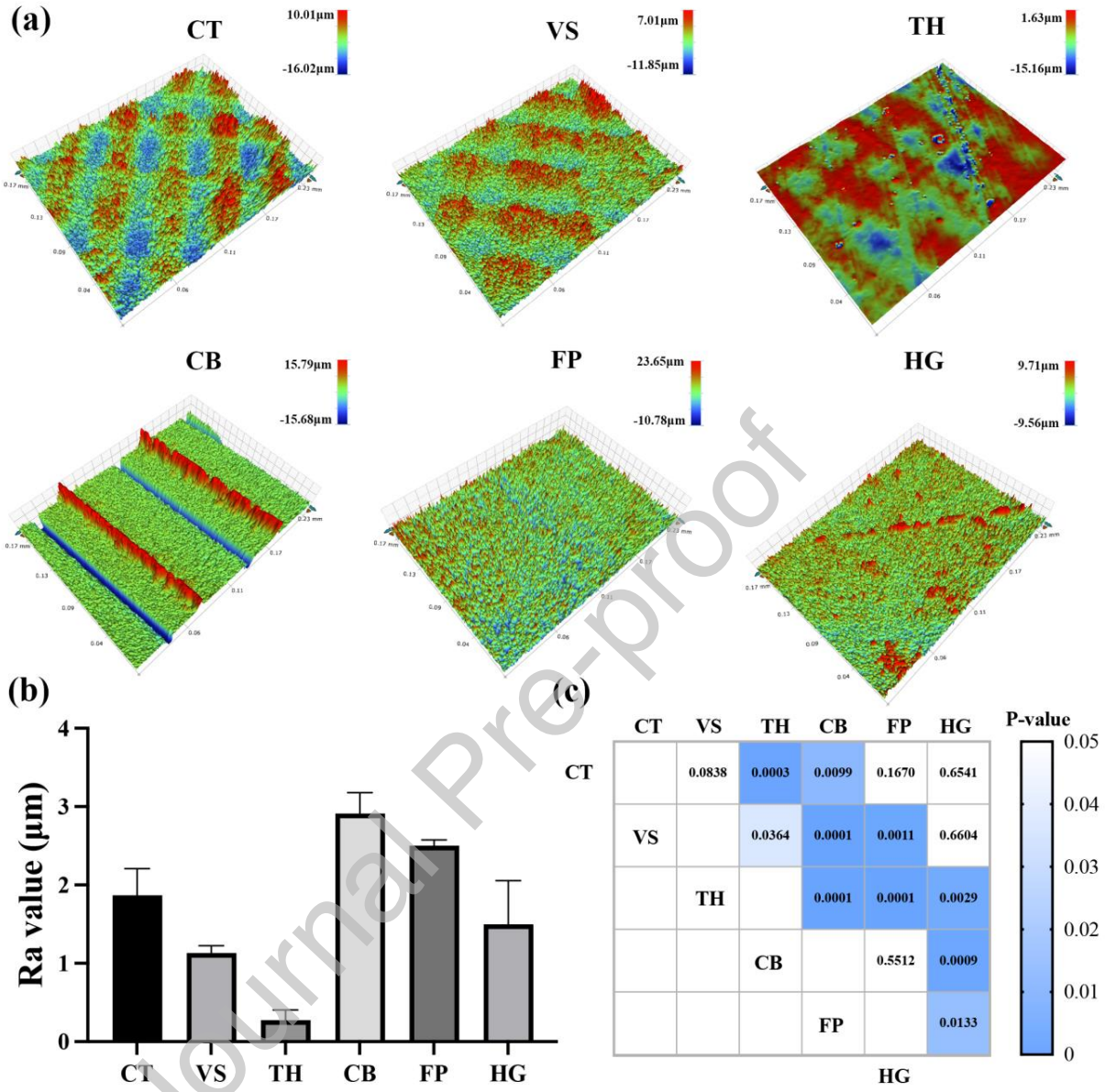

Fig 3

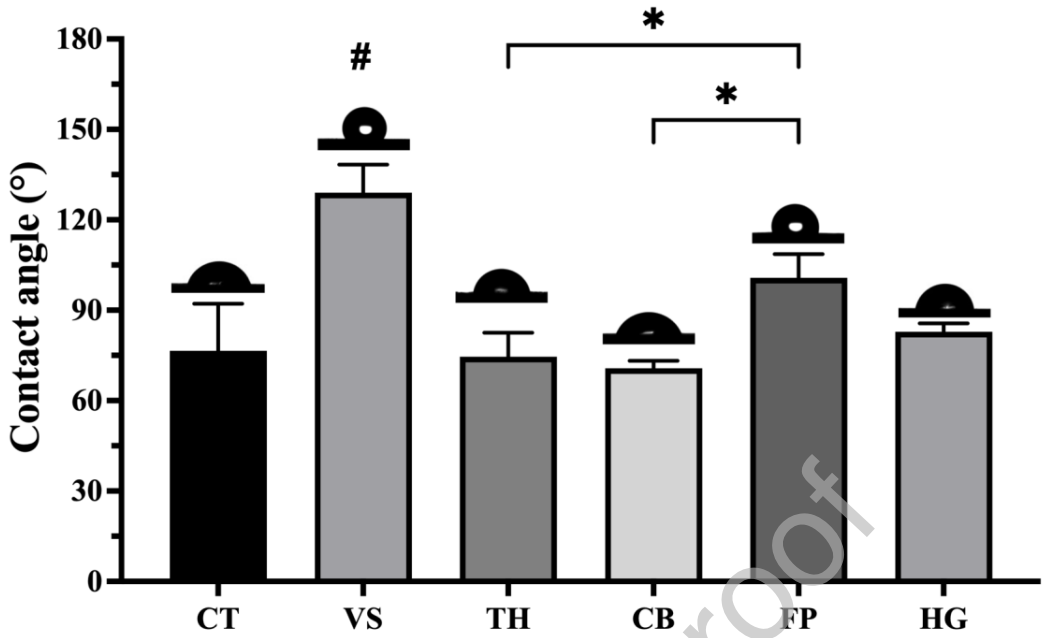

Fig 4

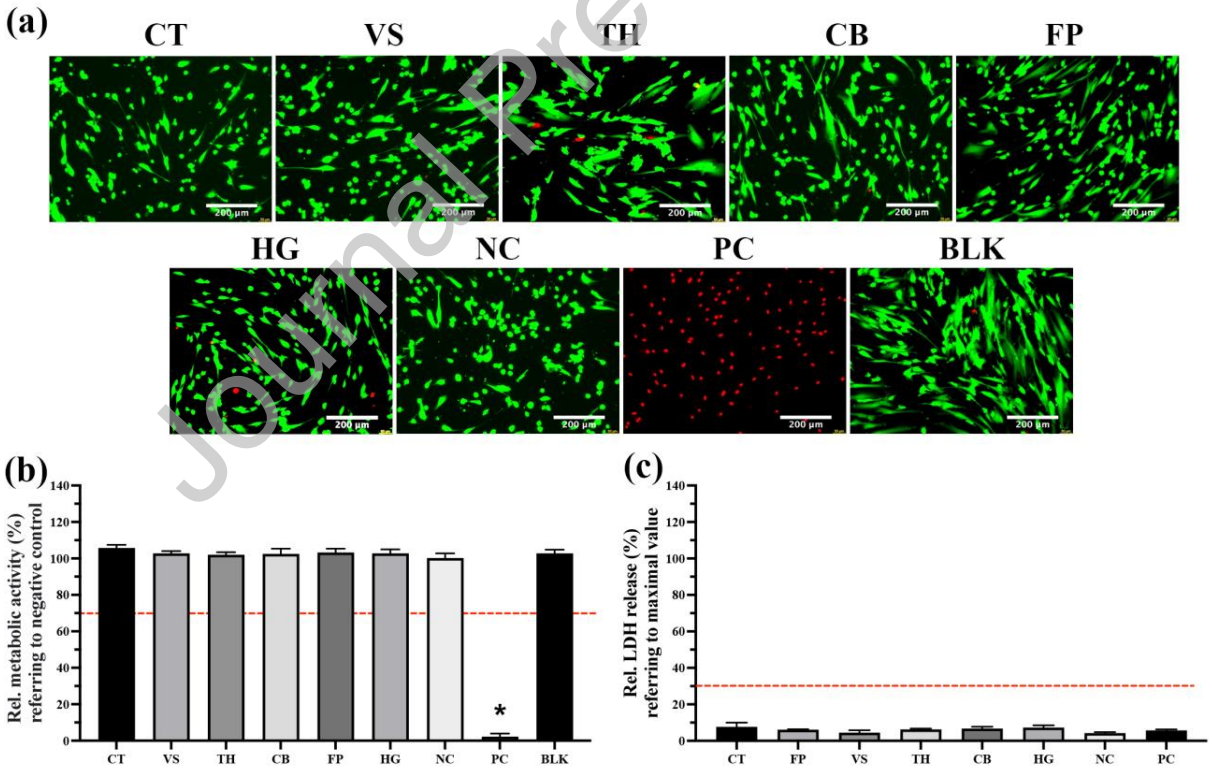

Fig 5

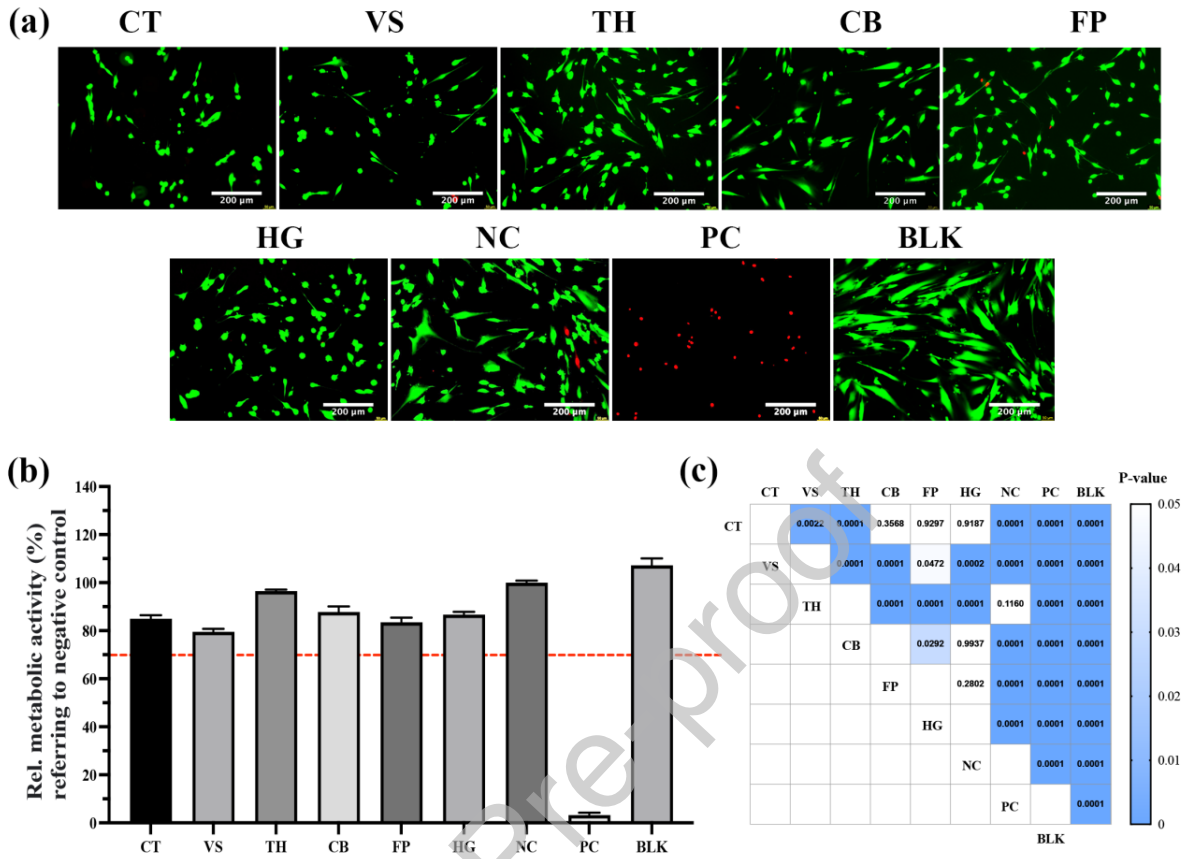

Fig 6

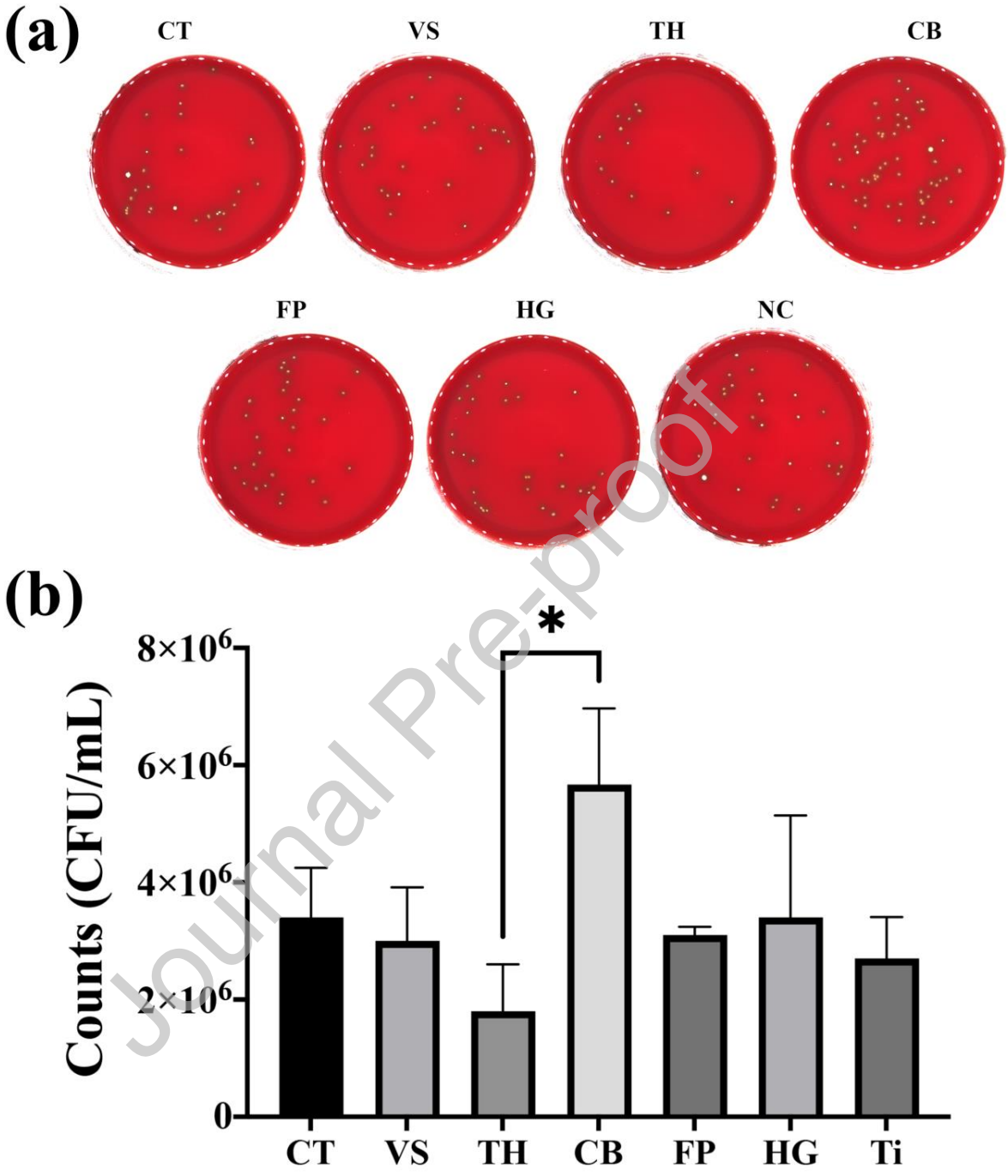

Fig 7

Conflict of interest

The authors report no conflict of interest regarding this manuscript.